

---

---

## ORIGINAL ARTICLE

---

---

# Contrast-Enhanced Ultrasound with Perfluorobutane for Hepatocellular Cancer Surveillance: Our Initial Local Experience

YS Chan<sup>1,2</sup>, CCM Cho<sup>1,2</sup>, TY Yuen<sup>1,2</sup>, HY Hung<sup>1,2</sup>, PKM Wong<sup>1</sup>, MMY Sou<sup>1</sup>, SSY Ho<sup>2</sup>,  
GLH Wong<sup>3</sup>, WCW Chu<sup>2</sup>

<sup>1</sup>Department of Imaging and Interventional Radiology, Prince of Wales Hospital, Hong Kong SAR, China

<sup>2</sup>Department of Imaging and Interventional Radiology, Faculty of Medicine, The Chinese University of Hong Kong, Hong Kong SAR, China

<sup>3</sup>Medical Data Analytic Centre, Department of Medicine and Therapeutics, Faculty of Medicine, The Chinese University of Hong Kong, Hong Kong SAR, China

### ABSTRACT

**Introduction:** Ultrasound is the most commonly used modality for hepatocellular cancer (HCC) surveillance in Hong Kong but has limitations in lesion characterisation. A second-generation perfluorobutane (PFB) ultrasound contrast agent allows for lesion characterisation through the usual vascular enhancement phases and provides an additional late Kupffer phase. We reviewed current evidence of PFB use in HCC care and investigated the value of contrast-enhanced ultrasound with PFB (PFB-CEUS) compared with brightness mode (B-mode) ultrasound in surveillance for HCC in high-risk patients in Hong Kong.

**Methods:** This prospective single-centre study assessed 50 high-risk patients under HCC surveillance undergoing B-mode ultrasound and PFB-CEUS, followed by gadoxetic acid-enhanced magnetic resonance imaging (MRI) within 3 weeks of the initial ultrasound scan. The MRI findings were considered the reference standard for the diagnosis of HCC. Detection rates of all and small ( $\leq 2$  cm) HCCs on both modalities and the adverse event rate for each modality were evaluated.

**Results:** The detection rate of small HCCs was 4% by B-mode ultrasound and 6% by PFB-CEUS. A total of four small HCCs were identified in our cohort. The immediate (day 0), short-term (day 7), and long-term (day 90) adverse event rates were 0%, 12% and 6%, respectively. All adverse events were mild and self-limiting, with an uncertain causal relationship to PFB administration.

**Conclusion:** PFB-CEUS is emerging as a useful imaging modality in evaluation of liver lesions and HCC detection. Our initial local experience provides positive agreement with the literature and identifies areas requiring further investigation.

**Key Words:** Carcinoma, hepatocellular; Diagnostic imaging; Liver neoplasms

---

---

**Correspondence:** Dr CCM Cho, Department of Imaging and Interventional Radiology, Prince of Wales Hospital, Hong Kong SAR, China

Email: [ccm193@ha.org.hk](mailto:ccm193@ha.org.hk)

Submitted: 11 October 2022; Accepted: 20 March 2023. This version may differ from the final version when published in an issue.

Contributors: CCMC, SSYH, GLHW and WCWC designed the study. CCMC, TYY, HYH, PKMW and MMYS acquired the data. YSC and PKMW analysed the data. YSC drafted the manuscript. All authors critically revised the manuscript for important intellectual content. All authors had full access to the data, contributed to the study, approved the final version for publication, and take responsibility for its accuracy and integrity.

Conflicts of Interest: GLHW has served as an advisory committee member for Gilead Sciences and Janssen, as a speaker for Abbot, AbbVie, Bristol Myers Squibb, Echosens, Furui, Gilead Sciences, Janssen and Roche, and received research grant from Gilead Sciences. As an editor of the journal, WCWC was not involved in the peer review process. Other authors have disclosed no conflicts of interest.

Funding/Support: This research received no specific grant from any funding agency in the public, commercial, or not-for-profit sectors.

Data Availability: All data generated or analysed during the present study are available from the corresponding author on reasonable request.

Ethics Approval: The research was approved by the Joint Chinese University of Hong Kong–New Territories East Cluster Clinical Research Ethics Committee (Ref No.: 2018.542) and was conducted in accordance with the Declaration of Helsinki and the International Conference on Harmonisation Good Clinical Practice. All patients gave informed consent for all treatments and procedures, and consent for publication.

## 中文摘要

### 以全氟丁烷對比增強超聲波監測肝細胞癌：我們的初步本地經驗

陳奕璇、曹子文、袁子祐、洪曉義、王嘉文、蘇妙怡、何倩儀、黃麗虹、朱昭穎

**簡介：**超聲波是香港最常使用的肝細胞癌監測方式，但在病變定性方面有其局限性。第二代全氟丁烷超聲波造影劑可通過通常的血管增強期來表徵病變，且提供額外的更晚的Kupffer期。我們回顧了目前全氟丁烷在肝細胞癌臨床處理的證據，並調查全氟丁烷對比增強超聲波與亮度模式（B模式）超聲波在監測本港肝細胞癌高風險患者方面的價值。

**方法：**本前瞻性單一中心研究評估了50名接受肝細胞癌監測的高風險患者，他們接受了B模式超聲波和全氟丁烷對比增強超聲波，隨後在初次超聲波掃描後3週內進行了釷塞酸增強磁力共振。磁力共振結果是診斷肝細胞癌的參考標準。我們評估了兩種模式下所有肝細胞癌和小肝細胞癌（≤2厘米）的檢出率以及不良事件發生率。

**結果：**B模式超聲波的小肝細胞癌檢出率為4%，全氟丁烷對比增強超聲波則為6%。我們的隊列中總共發現四宗小肝細胞癌。即時（第0天）、短期（第7天）和長期（第90天）不良事件發生率分別為0%、12%和6%。所有不良事件均為輕微且具有自限性，與全氟丁烷給藥之間的因果關係不確定。

**結論：**全氟丁烷對比增強超聲波正成為評估肝臟病變和肝細胞癌檢測的一種有用影像手段。我們最初的本地經驗與文獻一致，並確定了需要進一步研究的方向。

## INTRODUCTION

According to the Hong Kong Cancer Registry, hepatocellular carcinoma (HCC) is currently the fifth leading cancer and third leading cause of cancer deaths in Hong Kong despite the declining incidence of hepatitis B infection in recent years.<sup>1</sup> Chronic hepatitis B infection has an established association with, and is the major cause of, HCC. The latest territory-wide study performed in 2015 to 2016 showed a prevalence of 7.8% for hepatitis B infection in Hong Kong.<sup>2</sup> Many individuals with known infection are in imaging surveillance programmes, mostly using ultrasound as a screening tool.

Ultrasound is a relatively simple, radiation-free, widely available, low-cost imaging procedure with good patient acceptance. Ultrasound alone, however, is of limited sensitivity and is inadequate for an imaging diagnosis of HCC, which relies on the characteristic enhancement pattern of the lesion.<sup>3</sup>

### Basis of Ultrasound Contrast Agents and Technique of Contrast-Enhanced Ultrasound

The use of contrast-enhanced ultrasound dates back to 1969, when agitated normal saline was used in echocardiography, progressing to the wider application

of manufactured microbubbles in the 2000s to image different organs. Microbubbles are formed from an inert gas protected by an outer shell and are smaller than red blood cells. After intravenous injection, they can pass through the pulmonary capillaries and enter the systemic circulation. Being mainly extracellular blood pool agents, they stay in the vasculature, unlike iodinated contrast for computed tomography (CT) which is a soluble agent that will pass through vessel walls and can enter hepatocytes and the nephron. Both are able to provide information about the vascular pattern of the lesion of concern. The mechanism of action is that microbubbles increase the backscatter of ultrasound signal. They oscillate under ultrasound and the non-linear oscillations can cause harmonic emissions. These signals can be captured and processed to produce images with enhanced differentiation between vascular structures (with microbubbles within) and adjacent soft tissue.<sup>4</sup>

Currently, second-generation ultrasound contrast agents (UCAs) are in use worldwide. Commonly known second-generation UCAs include sulphur hexafluoride, which is used in Hong Kong, and perfluorobutane (PFB) which has been licensed in multiple countries for liver-specific imaging. Sonazoid (GE Healthcare, Milwaukee [WI], US) essentially contains PFB microbubbles

stabilised with a lipid coating with a well-defined diameter of approximately 3  $\mu\text{m}$ . Sonazoid to be used in imaging is prepared by reconstitution with 2-mL sterile water for injection. The usual recommended dose was 0.015 mL/kg. In addition to the standard vascular phases including arterial, portal venous and delayed phases, PFB has the unique ability to be taken up by the Kupffer cells. This enables Kupffer phase imaging which resembles the imaging obtained with a nuclear hepatobiliary scan. The microbubbles can stay in the Kupffer cells for up to a few hours. This aids in lesion detection and characterisation. During the Kupffer phase, the liver parenchyma should normally be uniformly enhancing; the presence of defects would indicate lesions devoid of Kupffer cells, allowing otherwise subtle lesions, in particular, lesions that may be isoechoic on brightness mode (B-mode) ultrasound, to become visible. Most malignancies, hepatic or metastatic, do not contain Kupffer cells, whereas benign entities such as focal nodular hyperplasia do contain such cells. This is comparable with using a liver-specific contrast agent such as gadoteric acid in magnetic resonance imaging (MRI) for hepatobiliary phase imaging. Leveraging this unique property of PFB, an imaging technique called defect reperfusion imaging was developed, using an additional contrast bolus injection for evaluation of the vascular characteristics of a defect in the Kupffer phase, further improving its diagnostic value.<sup>5</sup>

The time frames for the phases are as follows (assuming a normal cardiac output): the arterial phase starts at 10 seconds, peaks at 30 to 50 seconds, and is sustained until approximately 1 minute; the portovenous phase starts at 30 seconds, peaks at 80 to 90 seconds, and is sustained until approximately 2 minutes; the late vascular phase then ensues and is followed by the Kupffer phase (also called the post-vascular phase), which starts at approximately 10 minutes.<sup>6</sup>

### Perfluorobutane Applications

In 2008, the superiority of contrast-enhanced ultrasound with PFB (PFB-CEUS) versus unenhanced ultrasound in the diagnosis of focal liver lesions was confirmed by a phase III clinical trial by Miyamoto et al.<sup>7</sup> One study reported an even higher sensitivity and accuracy for PFB-CEUS than contrast-enhanced CT in detecting hepatic malignancy.<sup>8</sup> CEUS has value for lesions that are indeterminate on CT or MRI due to its heightened sensitivity in detecting vascular enhancement and real-time continuous evaluation of the enhancement pattern.<sup>9</sup> Compared with the other widely applied second-generation UCAs, several studies have confirmed

the non-inferiority of PFB.<sup>10,11</sup> A retrospective study published in 2010 by Kan et al<sup>12</sup> found a high sensitivity and specificity for detection of small ( $\leq 2$  cm) HCCs with additional tumours detected by PFB-CEUS compared with contrast-enhanced CT.

Beyond aiding initial imaging diagnosis, PFB has been found to increase the localisation rate of focal hepatic lesions for percutaneous biopsy.<sup>13,14</sup> Along the same lines, lesion localisation for radiofrequency ablation can also be improved, with a higher success rate and fewer treatment sessions required.<sup>15-17</sup>

Several studies have explored the utility of PFB in prediction of treatment response of HCC treated with transarterial chemoembolisation and other targeted therapies, using a reduction in lesion vascularity in an early post-intervention scan to predict the outcome.<sup>18-21</sup> In 2021, Funaoka et al<sup>22</sup> published their retrospective study testing the ability of PFB to evaluate the efficacy of radiotherapy for HCC, which further expands the potential indications of PFB-CEUS as the results were encouraging.

### Standardisation and Regulation

With the increasing recognition of PFB's utility, a consensus statement with guidelines for PFB's use was released in 2020 by the Asian Federation of Societies for Ultrasound in Medicine and Biology.<sup>6</sup> In the same year, the World Federation for Ultrasound in Medicine and Biology also published a good practice recommendation.<sup>9</sup> Part of the reporting standardisation of liver imaging is reliant on the use of the Liver Reporting and Data System (LI-RADS). The current version of LI-RADS, however, only applies to CEUS performed with sulphur hexafluoride microbubbles (Sonovue) and lipid-coated perfluoropropane microbubbles (Definity). An early study of a modified CEUS LI-RADS for PFB showed the LI-RADS categories LR-5 and LR-M to be good predictors of HCC and non-HCC malignancies.<sup>23</sup> A recent study also found no statistically significant difference between modified CEUS LI-RADS, CT, and the 2018 version of MRI LI-RADS in 31 histologically proven lesions.<sup>24</sup> Further inclusion of PFB is to be expected in the next version of CEUS LI-RADS, which can provide formal recognition of its value in HCC imaging.<sup>25</sup>

### Safety Consideration

PFB has an established low-risk profile. The incidence of adverse events was quoted to be 0.5% to 11.4%.<sup>6,26,27</sup>

No serious adverse events have been reported to date.<sup>6</sup> Common adverse effects include diarrhoea, proteinuria, and headache.<sup>6</sup> The overwhelming majority of these reported events did not require treatment.<sup>6,26,27</sup> Urticaria has been reported as an adverse effect. It must be noted that despite the lack of reported cases, anaphylaxis is a possible risk for any injectable agent. The most likely culprit for this potential allergic reaction is the lipid shell of PFB, which is derived from eggs. Therefore, egg allergy is the one and only contraindication to PFB use. Patients with renal insufficiency, or iodine or gadolinium contrast allergy, can undergo PFB-CEUS.

### Initial Local Experience

As PFB is an unregistered drug in Hong Kong, it is not currently in widespread use. We performed a pilot study to investigate the value of PFB-CEUS compared with conventional B-mode ultrasound for surveillance detection of HCC in high-risk patients.

## METHODS

### Design and Setting

This was a prospective, single-centre, single-arm study performed in Prince of Wales Hospital, a tertiary referral centre with hepatology and hepatobiliary surgery services available. The STARD (Standards for Reporting of Diagnostic Accuracy Studies) 2015 guidelines were used for reporting our results.

### Patient Recruitment

Patients were recruited by convenience sampling through clinician referral. A total of 50 patients were

recruited from the period 1 June 2020 to 3 May 2021. The inclusion and exclusion criteria are listed in Table 1.

### Imaging Workflow and Image Interpretation

Eligible patients were assessed via a standard workflow, starting with B-mode ultrasound and PFB-CEUS of the liver performed with the same settings, followed by MRI with gadoteric acid (Primovist; Bayer Schering Pharma, Berlin, Germany) within 3 weeks of the initial ultrasound scan (Figure 1). The B-mode ultrasound and PFB-CEUS were performed by two registered sonographers who have > 20 years of ultrasound experience, following standard technical specifications (Tables 2 and 3). Standard protocol was also implemented for the gadoteric acid-enhanced MRI (Table 4). The assessors were not blinded to clinical information of patients or past radiological investigations.

The findings of B-mode ultrasound, PFB-CEUS, and MRI were interpreted and reported separately by three radiologists who had > 5 years of experience in hepatobiliary imaging. As there were no standardised interpretation criteria for B-mode or PFB-CEUS in the diagnosis of HCC, interpretation of the findings from these two scans were based on a 3-point Likert scale (Table 5), while MRI findings were interpreted based on the 2018 version of LI-RADS.<sup>28</sup> The radiologists interpreting MRI were blinded to the results of ultrasound and vice versa. Any equivocal MRI findings were resolved by consensus between two radiologists subspecialising in hepatobiliary radiology. Those with negative findings on both PFB-CEUS and MRI, meaning no focal lesion or focal lesion(s) with low probability of HCC, followed the standard surveillance programme. Patients with intermediate probability for HCC were managed at the discretion of the referring team and underwent closer interval follow-up imaging or biopsy. Patients diagnosed with HCC were referred to the Joint Hepatoma Clinic of Prince of Wales Hospital for further management.

### Reference Standards

For patients undergoing hepatic surgery or biopsy, the final diagnosis was based on histological findings. For those who did not undergo surgery or biopsy, the diagnosis of HCC was based on MRI features fulfilling the LR-5 or LR-4 category of the 2018 version of LI-RADS.<sup>28</sup> They were managed in a similar manner in our clinical practice. For LR-3 lesions, which were not biopsied, additional follow-up CT or MRI was performed at the discretion of the referring clinical team.

**Table 1.** Inclusion and exclusion criteria for the study cohort.

Inclusion criteria	<ul style="list-style-type: none"> <li>- Age <math>\geq</math> 18 y</li> <li>- Known chronic liver disease with or without liver cirrhosis</li> <li>- Nodular liver parenchyma on ultrasonography</li> <li>- LSM-HCC score <math>\geq</math> 11 in chronic hepatitis B patients<sup>11</sup></li> <li>- LSM <math>\geq</math> 12.0 kPa in other chronic liver diseases<sup>2</sup></li> <li>- Informed written consent obtained</li> </ul>
Exclusion criteria	<ul style="list-style-type: none"> <li>- Child-Pugh score <math>\geq</math> 8</li> <li>- Previous or current HCC patients</li> <li>- Previous liver surgery</li> <li>- Liver transplantation</li> <li>- Contraindications to transient elastography (e.g., pregnancy, previous pacemaker implantation)</li> <li>- Contraindications to perfluorobutane contrast</li> <li>- Contraindications to gadoteric acid contrast</li> <li>- Contraindications to magnetic resonance imaging (e.g., metallic implants, pacemaker implantation)</li> <li>- Refusal to consent</li> </ul>

Abbreviations: HCC = hepatocellular carcinoma; LSM = liver stiffness measurement.

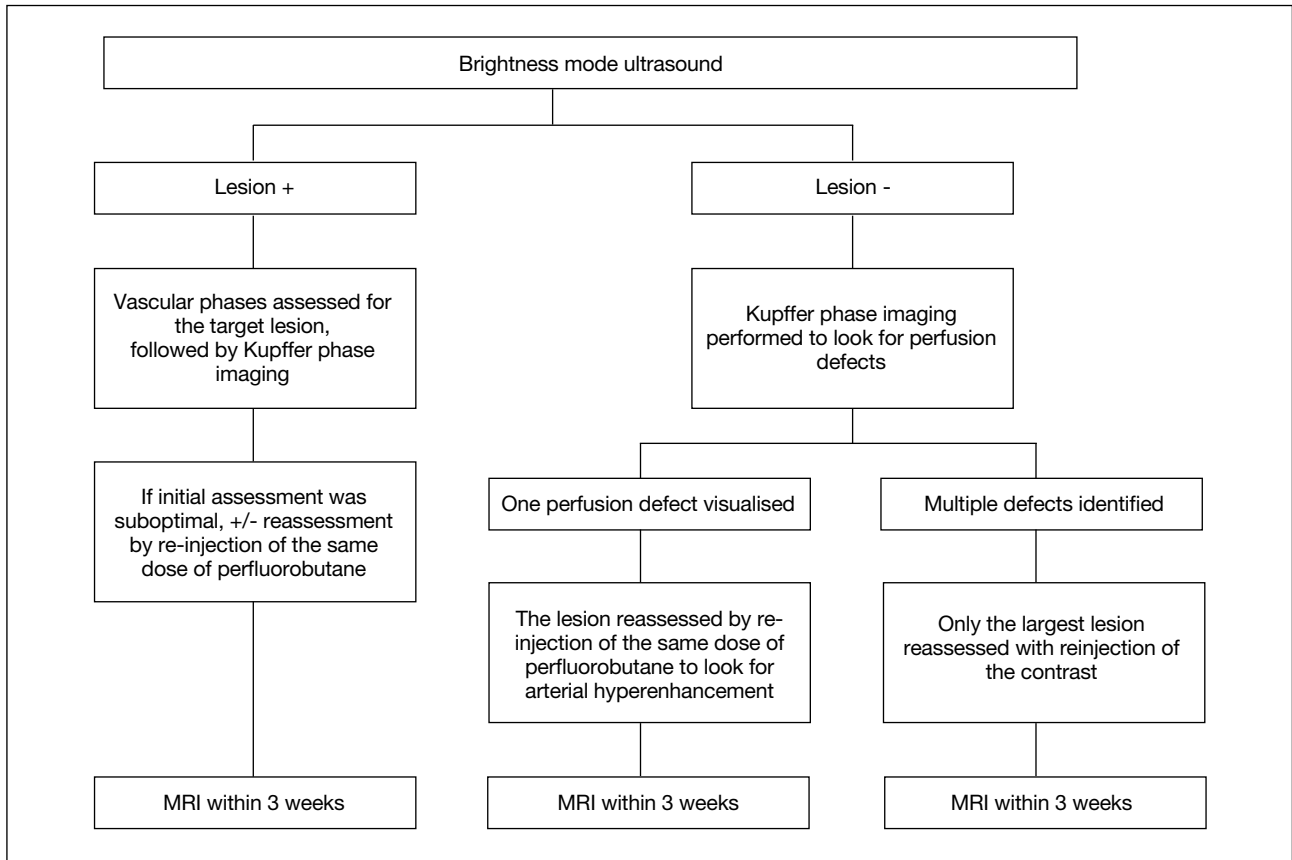


**Figure 1.** Imaging workflow for the study cohort. Abbreviation: MRI = magnetic resonance imaging.

**Table 2.** Technical specifications of brightness mode ultrasound.

Transducer	8-1 MHz curvilinear transducer of Canon Aplio i800 ultrasound system (Toshiba, Otawara, Japan)
Scanning approaches	Supine - Subcostal - Intercostal - Coronal Left lateral decubitus (supplementary) Left posterior oblique (supplementary)
Coverage	Entire liver
Brightness mode imaging	Liver size, parenchymal echotexture, surface, and any focal liver lesion
Colour Doppler imaging	Evaluation of patency of portal veins Evaluation of intralesional vascularity if focal liver lesion is detected

**Table 3.** Technical specifications of contrast-enhanced ultrasound with perfluorobutane.

Intravenous access	Antecubital or forearm vein
Contrast preparation	16 µg of perfluorobutane suspended in 2 mL of sterile water
Injection dose	0.015 mL/kg body weight
Injection method	Bolus with 10 mL saline flush
CEUS setting	
Scanning view	Dual view (brightness mode + contrast mode)
Mechanical index	0.20-0.26
Dynamic range	60-65 dB
Location of beam focus	Posterior margin of liver
Vascular phases	(after injection)
Arterial phase	10-20 seconds
Portal phase	30-45 seconds
Late phase	> 120 seconds
Post-vascular/Kupffer phase	10-15 minutes after contrast injection

Abbreviation: CEUS = contrast-enhanced ultrasound.

### Primary Endpoints

The primary endpoints were the detection rate of small ( $\leq 2$  cm) HCCs on B-mode US and PFB-CEUS. The detection rate was defined as the percentage of positive

findings on the respective imaging modality confirmed with a reference standard out of all patients in the study cohort. A positive finding was defined as a high-risk lesion on the Likert scale.

**Table 4.** Imaging protocol for magnetic resonance imaging with gadoxetic acid.

MRI scanner	3T scanner (Achieva; Philips Medical Systems, Eindhoven, the Netherlands)
Coil	Phase-array body coil
Sequences	
Pre-contrast T1W	Dual-echo axial T1W out-/in-phase gradient-echo images (TR/TE: 122/1.15 ms and 2.3 ms; FA: 70°)
T2W*	Respiratory-triggered single-shot T2W fast spin-echo 4-mm axial images with driven equilibrium (TR/TE: 838 ms/70 ms)
DWI*	DWI 5-mm axial images with b factors 0, 300 and 600
Multiphasic dynamic study	Three-dimensional axial T1W gradient-echo (TR/TE: 3.4 ms/1.7 ms; FA: 10°; matrix size: 211 × 172; field of view: 400 mm; No. of excitations: 1; slice thickness/gap: 4 mm/-2 mm; transverse slices: 100; for fat saturation: spectral pre-saturation with inversion recovery; parallel imaging factor: 3; scan time: 15.4 seconds)
Hepatobiliary phase imaging	T1W images with fat suppression
Contrast injection	Intravenous bolus injection of 25 µmol/kg (0.1 mL/kg) of gadoxetic acid (Primovist; Bayer Schering Pharma, Berlin, Germany) by means of a power injector at a rate of 1 mL/s, followed by 20 mL of saline chaser at the same rate during breath holding
Vascular phases	(after injection)
Arterial	30 seconds
Portal	70 seconds
Delayed	110 seconds
Late delayed	190 seconds
Hepatobiliary phase imaging	20 minutes

Abbreviations: DWI = diffusion-weighted imaging; FA = flip angle; MRI = magnetic resonance imaging; T1W = T1-weighted; T2W = T2-weighted; TE = echo time; TR = repetition time.

\* Performed during the 20-minute time gap before hepatobiliary phase imaging.

**Table 5.** Interpretation criteria for brightness mode ultrasound and perfluorobutane-enhanced ultrasound.

Risk of HCC	Brightness mode ultrasound	Perfluorobutane-enhanced ultrasound
Low	Ill-defined lesion with barely visible margin No or minimal vascularity	Isoenhancement with surrounding liver parenchyma in all vascular phases
Intermediate	Relatively well-defined lesion with discernible margin No or variable intralesional vascularity	Weak hyperenhancement in arterial phase No or mild washout in late vascular or Kupffer phase
High	Well-defined lesion with discernible or irregular margin Apparent/chaotic intralesional vascularity	Hyperenhancement in arterial phase with washout in vascular phase or washout in Kupffer phase

Abbreviation: HCC = hepatocellular cancer.

## Secondary Endpoints

The secondary endpoints included the detection rate of all sizes of HCC and immediate (day 0), short-term (day 7) and long-term (day 90) adverse event rates. Adverse events were recorded according to the CTCAE (Common Terminology Criteria for Adverse Events) version 5.0 with structured telephone interviews at 1 week and 90 days after the ultrasound examination.<sup>29</sup>

## RESULTS

A total of 50 patients were included in the study, consisting of 32 men and 18 women with a mean age of 62.6 years (Table 6). The majority (72%) of the patients

were in the HCC surveillance programme due to hepatitis B. All of the patients had had prior surveillance imaging. For 94% of the patients, the previous surveillance scans were B-mode ultrasound while the rest were contrast-enhanced CT. The median time from prior surveillance imaging to ultrasound evaluation our study was 12.5 months. The median time from PFB-CEUS to MRI was 11 days. None of the detected lesions underwent biopsy or surgical resection during the study period.

## Primary Endpoints

The detection rates of small HCCs were 4% (n = 2) by B-mode ultrasound and 6% (n = 3) by PFB-CEUS. A

total of four small HCCs were identified in our cohort (Table 7). Figures 2 to 5 show the key imaging features of these four HCCs found in our cohort.

### Secondary Endpoints

There was no HCC > 2 cm identified in the study cohort. The immediate adverse event rate was 0%, the short-term adverse event rate was 12% (n = 6), and the long-term adverse event rate was 6% (n = 3) [Table 8]. All of the adverse events were mild and self-limiting, with an uncertain causal relationship to PFB administration.

## DISCUSSION

In our study, PFB-CEUS had a slightly better detection

rate of HCC than B-mode ultrasound. Although all of the HCCs were detectable by either modality, B-mode ultrasound falsely classified two of the lesions as intermediate risk on the Likert scale, while PFB-CEUS was able to add value by reclassifying one of these lesions underclassified by B-mode ultrasound as a high-risk lesion. This finding is in keeping with that of Park et al,<sup>30</sup> though no statistical significance was identified in their study for the detection of additional small HCCs by PFB-CEUS.

With this initial trial of PFB application, we have learned a few lessons in its use. First of all, deep lesions are difficult to evaluate by PFB-CEUS. The one false-negative lesion on PFB-CEUS was a lesion located deep in the parenchyma, 9 cm from the skin surface (Figure 3). The difficulty of evaluating deep lesions by PFB-CEUS was recognised due to ultrasound attenuation in low mechanical index settings.<sup>6</sup> Although switching to high mechanical index settings in B-mode ultrasound can aid assessment, the limited assessment by PFB-CEUS precludes its value addition in deep lesion characterisation.

In addition to the technical aspect of PFB use, we made an observation of a unique property. One of the LR-4 lesions was identified in the Kupffer phase as a defect on PFB-CEUS, while showing hyperintensity on the hepatobiliary phase in gadoxetic acid-enhanced MRI. This evokes a complex discussion involving both PFB, liver-specific MRI contrast properties and HCC cell biology. PFB-CEUS has often been compared with gadoxetic acid-enhanced MRI for its characteristic liver-specific phase—the Kupffer phase. The two phases share similarities by predominantly identifying HCC as focal defects, but have fundamentally different principles underlying them. For gadoxetic acid-enhanced MRI, the hepatobiliary phase appearance is based upon the organic anion transporting polypeptide 8 (*OATP8*)

**Table 6.** Patient demographics (n = 50).\*

Sex	
Male	32 (64%)
Female	18 (36%)
Mean age, y (range) <sup>†</sup>	62.6 (41-86)
Body mass index	18.3-49.5
Albumin level, g/L	24-47
Bilirubin level, µmol/L	5-45
Alpha fetoprotein level, µg/mL	1-12
Cause of surveillance	
Hepatitis B	36 (72%)
Hepatitis C	3 (6%)
Hepatitis B and alcoholic cirrhosis	2 (4%)
Autoimmune hepatitis	6 (12%)
Hepatitis B and autoimmune hepatitis	1 (2%)
Primary biliary cholangitis	1 (2%)
Cryptogenic cirrhosis	1 (2%)
Current antiviral treatment	
Yes	38 (76%)
No	12 (24%)
Child-Pugh class	
A	10 (20%)
B	6 (12%)
C	2 (4%)
Unclassified	32 (64%)

\* Data are shown as No. (%) or range, unless otherwise specified.

<sup>†</sup> Mean age of male: 61.7; mean age of female: 64.1.

**Table 7.** Characteristics of hepatocellular cancer detected in the study cohort.

Case No.		Cause of surveillance	Location	Size, mm	Likert scale on B-mode US	Likert scale on PFB-CEUS	MRI LI-RADS	Management	Figure
3	Lesion 1	Primary biliary cholangitis	S6	13	Intermediate	High	5	MWA	2
12	Lesion 1	Hepatitis B	S5	19	High	High	4	Palliative care	3
23		Hepatitis B	S8	10	Intermediate	Intermediate	4	MWA	4
40		Hepatitis B	S3	16	High	High	4	Palliative care	5

Abbreviations: B-mode US = brightness mode ultrasound; LI-RADS = Liver Reporting and Data System; MRI = magnetic resonance imaging; MWA = microwave ablation; PFB-CEUS = contrast-enhanced ultrasound with perflurobutane; S3 = segment 3; S5 = segment 5; S6 = segment 6; S8 = segment 8.

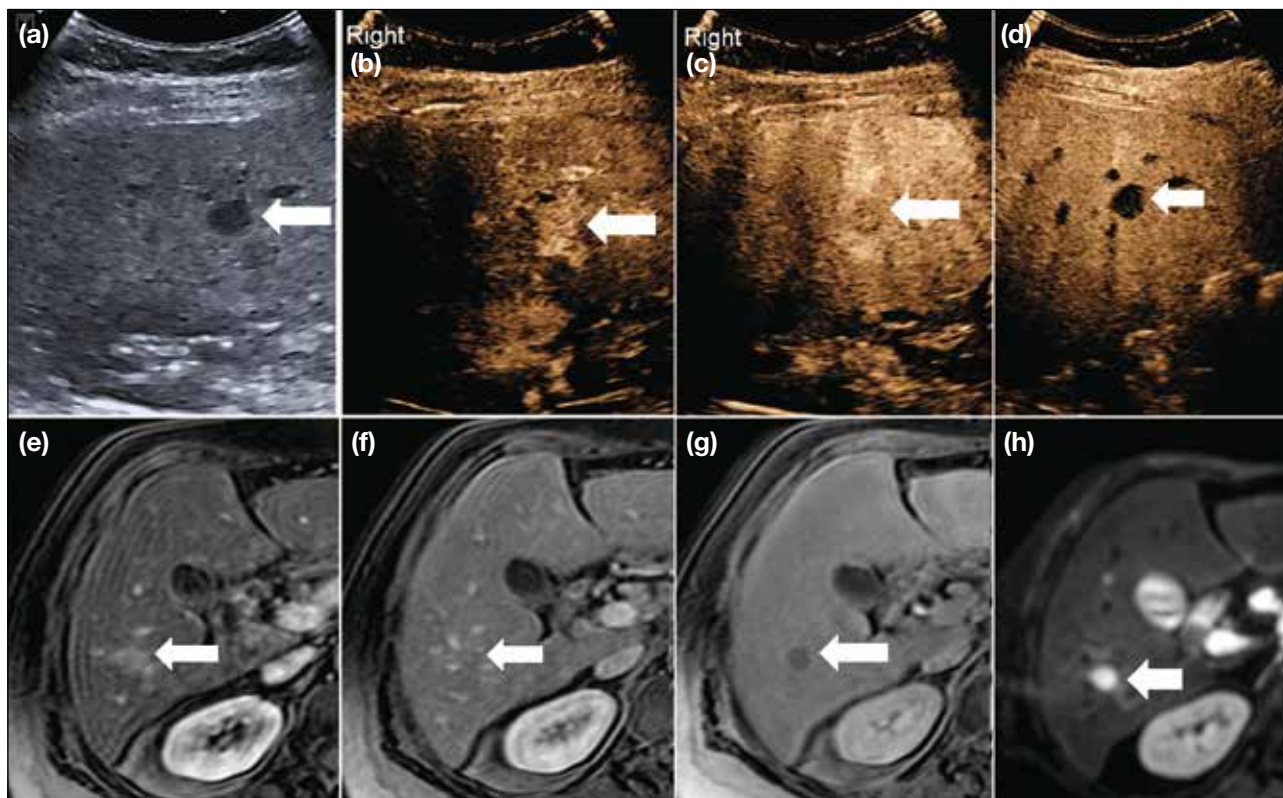


**Figure 2.** A hepatocellular carcinoma (arrows) in a patient with underlying primary biliary cholangitis. (a) Brightness mode ultrasound showing a well-defined round hypoechoic lesion. Perflurobutane-enhanced ultrasound images in (b) arterial, (c) portovenous, and (d) Kupffer phases showing the lesion to be arterial hyperenhancing in the arterial phase, with portovenous washout and a Kupffer phase defect. T1-weighted fat-saturated axial gadoteric acid-enhanced magnetic resonance imaging images in (e) arterial and (f) portovenous phases showing corresponding enhancing pattern. (g) Hepatobiliary phase image showing corresponding focal defect. (h) Diffusion-weighted imaging (DWI) image showing high DWI value, with corresponding low apparent diffusion coefficient value (not shown) in keeping with restricted diffusion.

expression of cells. Normal hepatocytes take up contrast through *OATP*, while both early and progressed HCCs often have a reduced expression of *OATP* during hepatocarcinogenesis, reducing their contrast uptake in the hepatobiliary phase, leading to a hepatobiliary phase defect.<sup>31</sup> Hepatobiliary phase-hyperintense HCC is, however, not uncommon, constituting up to 10% of cases.<sup>32</sup> It has been suggested that hepatobiliary phase hyperintensity may be seen in some moderately- or well-differentiated HCCs, but has been reported in poorly differentiated HCC as well and is due to paradoxical upregulation of *OATP*.<sup>33</sup> On the other hand, for PFB-CEUS, the contrast between normal parenchyma and HCC is achieved by differences in the number of Kupffer cells. Kupffer cells are liver-specific macrophages, which phagocytose the microbubbles, causing enhancement of hepatic parenchyma. The Kupffer cell count is seen to decline with hepatocarcinogenesis and

has been suggested to decline more slowly than *OATP8* expression.<sup>32</sup> The presence of a Kupffer phase defect strongly suggests progression of HCC. Korenaga et al<sup>34</sup> found that all the moderately and poorly differentiated HCCs in their study showed Kupffer phase defects while well-differentiated HCCs tended to lack them. Our LR-4 lesion did not undergo histological confirmation, but we speculated that it is a moderately differentiated HCC based on the uptake. Further studies are warranted to look into the potential use of PFB-CEUS versus gadoteric acid-enhanced MRI for predicting the histological differentiation of HCC.

We have also identified a potential advantage of using PFB-CEUS, which is in patients with hepatic iron overload. One of the patients was found to have heavy iron deposition on MRI. This markedly impaired the assessment on hepatobiliary phase as the whole



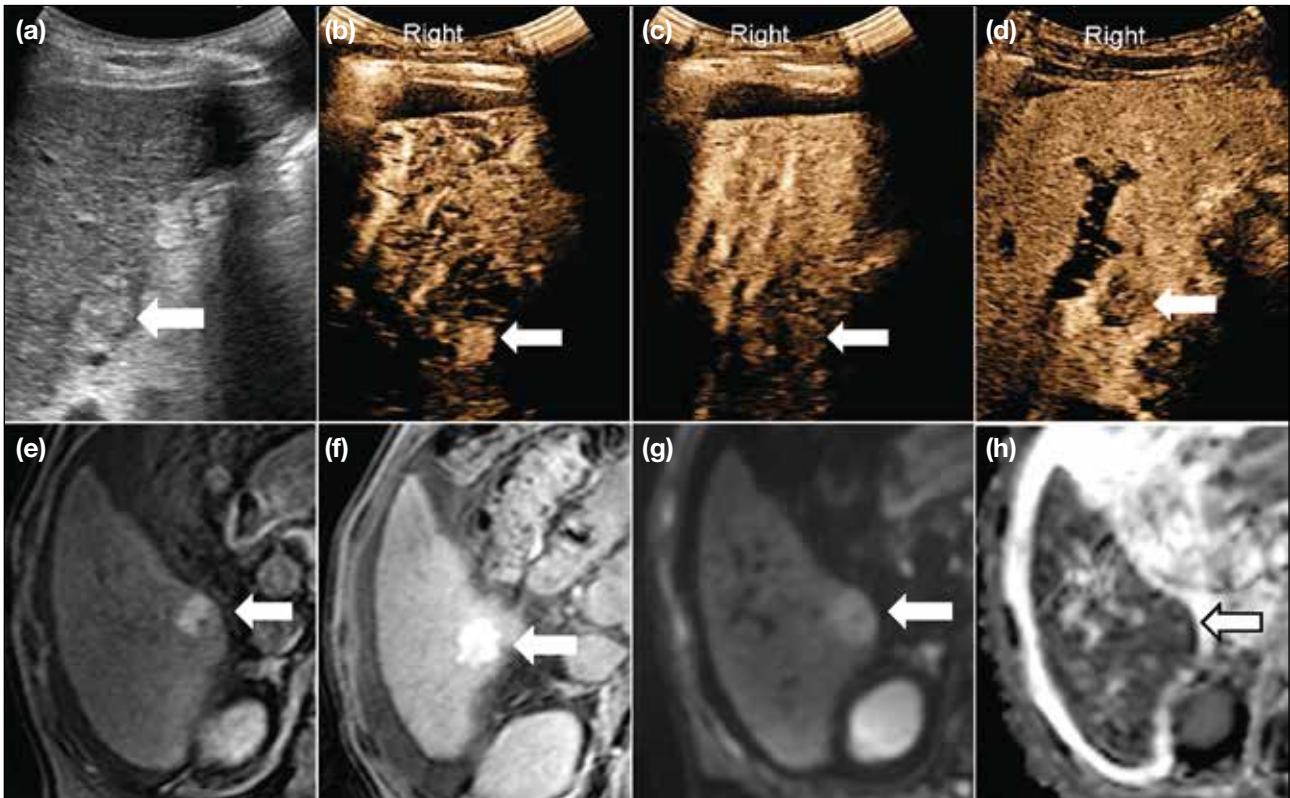


**Figure 3.** A hepatocellular carcinoma (arrows) in a patient with chronic hepatitis B infection. (a) Brightness mode ultrasound identified a well-defined hyperechoic lesion. Perfluorobutane-enhanced ultrasound in (b) arterial, (c) portovenous, and (d) Kupffer phases identified characteristic pattern of arterial hyperenhancement, portovenous washout with a Kupffer phase defect. (e) T1-weighted fat-saturated axial gadoteric acid-enhanced magnetic resonance imaging image showing arterial hyperenhancement of the lesion. (f) Hepatobiliary phase image showing hepatobiliary phase uptake of the lesion. (g) Diffusion-weighted image and (h) apparent diffusion coefficient map confirmed restricted diffusion in the lesion.

liver remained hypointense due to iron deposition. Iron overload is a recognised risk factor for HCC development. Due to the paramagnetic effect of iron, iron-overloaded liver parenchyma shows markedly hypointense signal on T1-weighted and T2-weighted images, providing excellent contrast for iron-sparing HCC. It should be noted, however, that siderotic nodules may also be found in such patients. Siderotic nodules are hypointense, making them inconspicuous due to a similar hypointense appearance to the surrounding liver tissue which is also iron-overloaded. With the similar liver-specific nature of PFB and liver-specific MRI contrast, we pondered the possibility of the superiority of use of PFB-CEUS in iron-overloaded liver in demonstrating a liver-specific phase defect. Up to now, the effect of hepatic iron overload on Kupffer cell function and Kupffer phase defects for HCC detection has not been described. Our study has identified a unique area in PFB-

CEUS use that has not been previously described, and further investigation into the use of PFB-CEUS Kupffer phase imaging as an alternative screening method for patients with hepatic iron overload should be carried out. This also brings out the possibility of using PFB-CEUS in other conditions where the hepatobiliary phase assessment on MRI is limited, e.g., patients with poor hepatic function, severe cirrhosis, or cholestasis.<sup>30</sup>

### Limitation

The main limitation of our study is the small sample size and low incidence of HCC in our cohort, which limits the potential for statistical evaluation. This study framework served more as a standardised approach to our initial experience with PFB use in HCC surveillance. Despite the small size, we were able to identify a few points in the use of PFB that require further development and found additional value of PFB use that is in keeping with

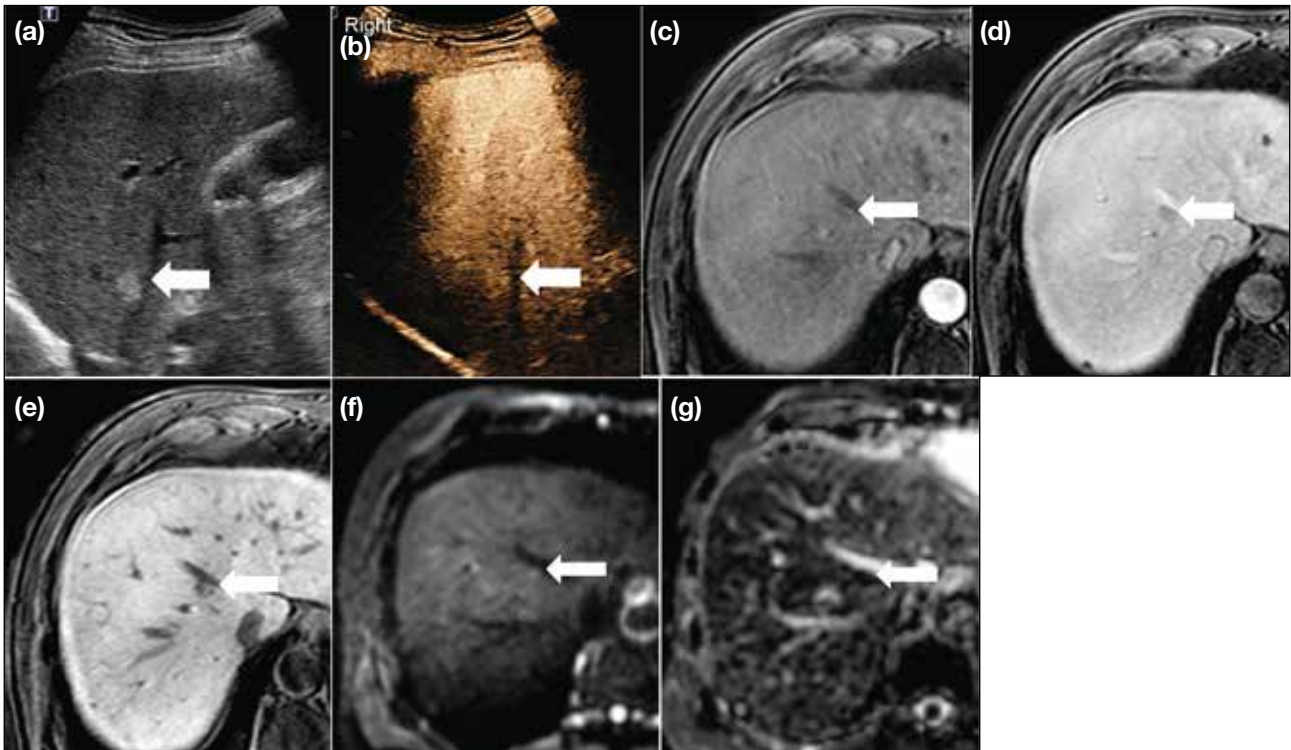


**Figure 4.** A hepatocellular carcinoma (HCC) [arrows] in a patient with hepatitis B. The HCC was seen as a deep-seated well-defined hyperechoic lesion on brightness mode ultrasound (a), with subtle corresponding arterial hyperenhancement on perfluorobutane-enhanced ultrasound (b). The deep-seated location rendered assessment difficult in subsequent phases. T1-weighted fat-saturated gadoteric acid-enhanced magnetic resonance imaging image in arterial phase (c) did not reveal any abnormal enhancement, but a focal lesion abutting the middle hepatic vein was seen to washout on portovenous phase (d), with corresponding defect on hepatobiliary phase (e). Faint restricted diffusion was evident with focal hyperintensity at the corresponding site diffusion-weighted imaging MRI on (f) and hypointensity on apparent diffusion coefficient image (g).

findings in the literature. Further studies with a larger sample size may be attempted to allow for statistical evaluation of this slowly maturing modality of choice.

## CONCLUSION

PFB-CEUS is an emerging imaging modality in evaluation of liver lesions and HCC detection, with increased recognition worldwide and expanding potential uses. Our initial local experience provides positive agreement with the literature and identified areas requiring further investigation, including correlation of Kupffer phase defects and hepatobiliary phase defects with histological differentiation, and potential use of the Kupffer phase in assessment of patients with iron-overloaded livers.

## REFERENCES

1. Hospital Authority. Overview of Hong Kong Cancer Statistics of 2019. 2021. Available from: <https://www3.ha.org.hk/cancereg/pdf/>

overview/Overview%20of%20HK%20Cancer%20Stat%202019.pdf. Accessed 27 Feb 2024.

- Liu KS, Seto WK, Lau EH, Wong DK, Lam YF, Cheung KS, et al. A territorywide prevalence study on blood-borne and enteric viral hepatitis in Hong Kong. *J Infect Dis.* 2019;219:1924-33.
- Chou R, Cuevas C, Fu R, Devine B, Wasson N, Ginsburg A, et al. Imaging techniques for the diagnosis of hepatocellular carcinoma: a systematic review and meta-analysis. *Ann Intern Med.* 2015;162:697-711.
- Baun J. Contrast-enhanced ultrasound: a technology primer. *J Diagn Med Sonogr.* 2017;33:446-52.
- Kudo M, Hatanaka K, Maekawa K. Newly developed novel ultrasound technique, defect reperfusion ultrasound imaging, using Sonazoid in the management of hepatocellular carcinoma. *Oncology.* 2010;78 Suppl 1:40-5.
- Lee JY, Minami Y, Choi BI, Lee WJ, Chou YH, Jeong WK, et al. The AFSUMB consensus statements and recommendations for the clinical practice of contrast-enhanced ultrasound using Sonazoid. *Ultrasonography.* 2020;39:191-220.
- Miyamoto Y, Ito T, Takada E, Omoto K, Hirai T, Moriyasu F. Efficacy of Sonazoid (perflubutane) for contrast-enhanced ultrasound in the differentiation of focal breast lesions: phase 3 multicenter clinical trial. *AJR Am J Roentgenol.* 2014;202:W400-7.

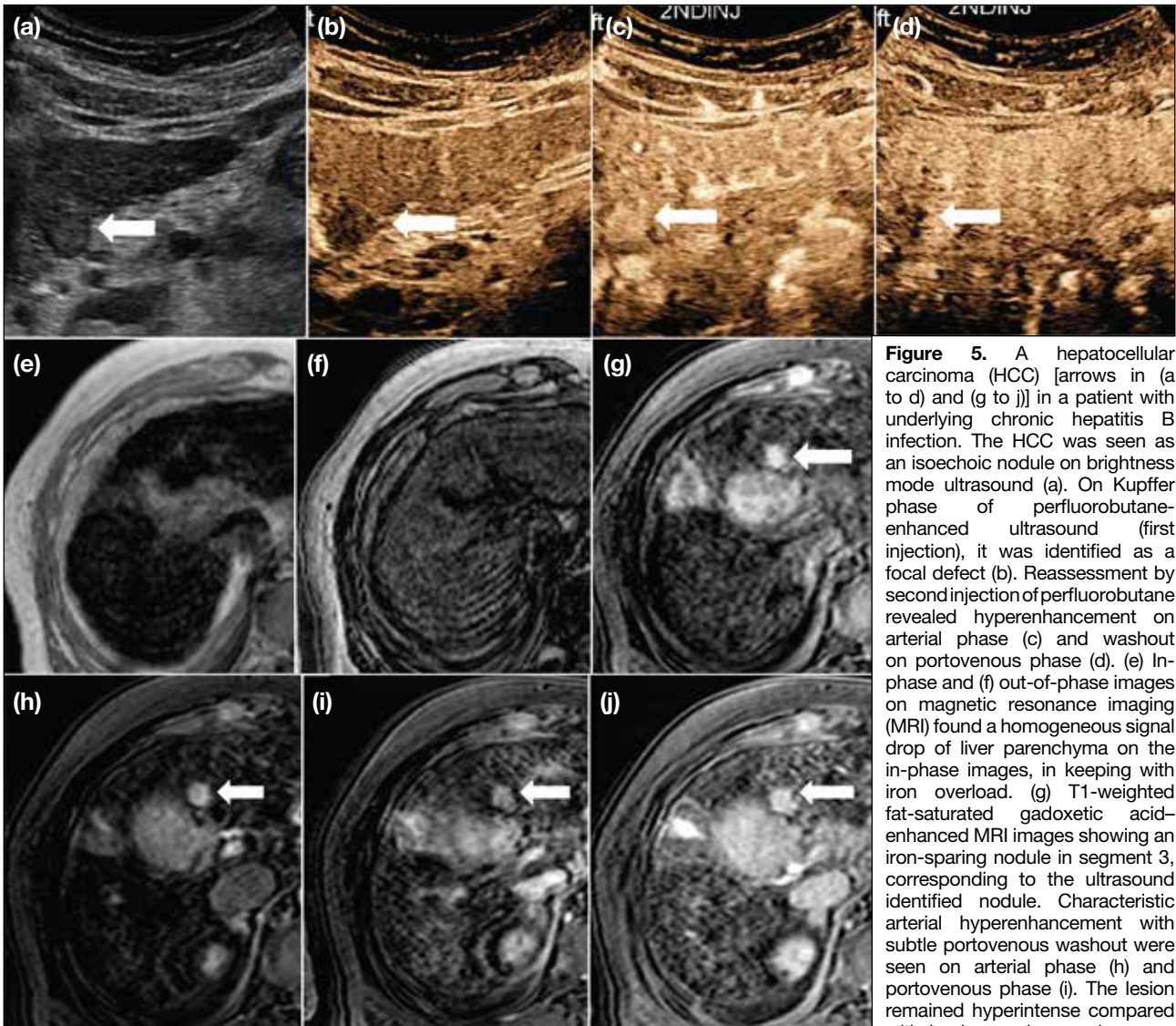


**Figure 5.** A hepatocellular carcinoma (HCC) [arrows in (a to d) and (g to j)] in a patient with underlying chronic hepatitis B infection. The HCC was seen as an isoechoic nodule on brightness mode ultrasound (a). On Kupffer phase of perfluorobutane-enhanced ultrasound (first injection), it was identified as a focal defect (b). Reassessment by second injection of perfluorobutane revealed hyperenhancement on arterial phase (c) and washout on portovenous phase (d). (e) In-phase and (f) out-of-phase images on magnetic resonance imaging (MRI) found a homogeneous signal drop of liver parenchyma on the in-phase images, in keeping with iron overload. (g) T1-weighted fat-saturated gadoxetic acid-enhanced MRI images showing an iron-sparing nodule in segment 3, corresponding to the ultrasound identified nodule. Characteristic arterial hyperenhancement with subtle portovenous washout were seen on arterial phase (h) and portovenous phase (i). The lesion remained hyperintense compared with background parenchyma on the hepatobiliary phase image (j).

**Table 8.** Adverse events.\*

	Day 7 No. of patients (Grade)	Day 90 No. of patients (Grade)	Duration
Injection site pain	1 (1)	0	N/A
Sore throat	1 (1)	0	2 days
Cough	1 (1)	0	2 days
Hand stiffness	1 (1)	0	2 hours
Leg cramp	0	1 (1)	Once
Anal pain	1 (1)	0	1 week
Gastrointestinal discomfort	1 (2)	1 (1)	1 week
Malaise	0	1 (1)	N/A

Abbreviation: N/A = not available.

\* No immediate adverse event was recorded.

8. Hatanaka K, Kudo M, Minami Y, Maekawa K. Sonazoid-enhanced ultrasonography for diagnosis of hepatic malignancies: comparison with contrast-enhanced CT. *Oncology*. 2008;75 Suppl 1:42-7.
9. Dietrich CF, Nolsøe CP, Barr RG, Berzigotti A, Burns PN, Cantisani V, et al. Guidelines and good clinical practice recommendations for contrast-enhanced ultrasound (CEUS) in the liver—update 2020—WFUMB in cooperation with EFSUMB, AFSUMB, AIUM, and FLAUS. *Ultraschall Med*. 2020;41:562-85.
10. Zhai HY, Liang P, Yu J, Cao F, Kuang M, Liu FY, et al. Comparison of Sonazoid and SonoVue in the diagnosis of focal liver lesions: a preliminary study. *J Ultrasound Med*. 2019;38:2417-25.
11. Lv K, Zhai H, Jiang Y, Liang P, Xu HX, Du L, et al. Prospective assessment of diagnostic efficacy and safety of Sonazoid™ and SonoVue® ultrasound contrast agents in patients with focal liver lesions. *Abdom Radiol (NY)*. 2021;46:4647-59.
12. Kan M, Hiraoka A, Uehara T, Hidaka S, Ichiryu M, Nakahara H,

- et al. Evaluation of contrast-enhanced ultrasonography using perflurobutane (Sonazoid®) in patients with small hepatocellular carcinoma: comparison with dynamic computed tomography. *Oncol Lett.* 2010;1:485-8.
13. Eso Y, Takai A, Takeda H, Matsumoto T, Lee M, Inuzuka T, et al. Sonazoid-enhanced ultrasonography guidance improves the quality of pathological diagnosis in the biopsy of focal hepatic lesions. *Eur J Gastroenterol Hepatol.* 2016;28:1462-7.
  14. Park HS, Kim YJ, Yu MH, Jung SI, Jeon HJ. Real-time contrast-enhanced sonographically guided biopsy or radiofrequency ablation of focal liver lesions using perflurobutane microbubbles (Sonazoid): value of Kupffer-phase imaging. *J Ultrasound Med.* 2015;34:411-21.
  15. Minami Y, Kudo M, Hatanaka K, Kitai S, Inoue T, Hagiwara S, et al. Radiofrequency ablation guided by contrast harmonic sonography using perfluorocarbon microbubbles (Sonazoid) for hepatic malignancies: an initial experience. *Liver Int.* 2010;30:759-64.
  16. Masuzaki R, Shiina S, Tateishi R, Yoshida H, Goto E, Sugioka Y, et al. Utility of contrast-enhanced ultrasonography with Sonazoid in radiofrequency ablation for hepatocellular carcinoma. *J Gastroenterol Hepatol.* 2011;26:759-64.
  17. Dohmen T, Kataoka E, Yamada I, Miura K, Ohshima S, Shibuya T, et al. Efficacy of contrast-enhanced ultrasonography in radiofrequency ablation for hepatocellular carcinoma. *Intern Med.* 2012;51:1-7.
  18. Shiozawa K, Watanabe M, Kikuchi Y, Kudo T, Maruyama K, Sumino Y. Evaluation of sorafenib for hepatocellular carcinoma by contrast-enhanced ultrasonography: a pilot study. *World J Gastroenterol.* 2012;18:5753-8.
  19. Sugimoto K, Moriyasu F, Saito K, Rognin N, Kamiyama N, Furuichi Y, et al. Hepatocellular carcinoma treated with sorafenib: early detection of treatment response and major adverse events by contrast-enhanced US. *Liver Int.* 2013;33:605-15.
  20. Xia Y, Kudo M, Minami Y, Hatanaka K, Ueshima K, Chung H, et al. Response evaluation of transcatheter arterial chemoembolization in hepatocellular carcinomas: the usefulness of Sonazoid-enhanced harmonic sonography. *Oncology.* 2008;75 Suppl 1:99-105.
  21. Kono Y, Lucidarme O, Choi SH, Rose SC, Hassanein TI, Alpert E, et al. Contrast-enhanced ultrasound as a predictor of treatment efficacy within 2 weeks after transarterial chemoembolization of hepatocellular carcinoma. *J Vasc Interv Radiol.* 2007;18:57-65.
  22. Funaoka A, Numata K, Takeda A, Saigusa Y, Tsurugai Y, Nihonmatsu H, et al. Use of contrast-enhanced ultrasound with Sonazoid for evaluating the radiotherapy efficacy for hepatocellular carcinoma. *Diagnostics (Basel).* 2021;11:486.
  23. Sugimoto K, Kakegawa T, Takahashi H, Tomita Y, Abe M, Yoshimasu Y, et al. Usefulness of modified CEUS LI-RADS for the diagnosis of hepatocellular carcinoma using Sonazoid. *Diagnostics (Basel).* 2020;10:828.
  24. Hwang JA, Jeong WK, Min JH, Kim YY, Heo NH, Lim HK. Sonazoid-enhanced ultrasonography: comparison with CT/MRI liver imaging reporting and data system in patients with suspected hepatocellular carcinoma. *Ultrasonography.* 2021;40:486-98.
  25. Minami Y, Kudo M. Contrast-enhanced ultrasonography with Sonazoid in hepatocellular carcinoma diagnosis. *Hepatoma Res.* 2020;6:46.
  26. Miyamoto Y, Ito T, Takada E, Omoto K, Hirai T, Moriyasu F. Efficacy of Sonazoid (perflubutane) for contrast-enhanced ultrasound in the differentiation of focal breast lesions: phase 3 multicenter clinical trial. *AJR Am J Roentgenol.* 2014;202:W400-7.
  27. Mori Y, Hayakawa A, Abe K, Tanigawa M, Takahashi M, Naruse H, et al. The safety and the efficacy of ultrasound contrast media perflubutane microbubbles in clinical practice. *Choonpa Igaku.* 2011;38:541-48.
  28. American College of Radiology Committee on LI-RADS. CT/MRI LI-RADS® v2018 CORE. Available from: <https://www.acr.org/-/media/ACR/Files/RADS/LI-RADS/LI-RADS-2018-Core.pdf>. Accessed 17 Jul 2022.
  29. Department of Health and Human Services, United States Government. Common Terminology Criteria for Adverse Events (CTCAE) Version 5.0. 2017. Available from: [https://ctep.cancer.gov/protocoldevelopment/electronic\\_applications/docs/ctcae\\_v5\\_quick\\_reference\\_5x7.pdf](https://ctep.cancer.gov/protocoldevelopment/electronic_applications/docs/ctcae_v5_quick_reference_5x7.pdf). Accessed 2 May 2022.
  30. Park JH, Park MS, Lee SJ, Jeong WK, Lee JY, Park MJ, et al. Contrast-enhanced US with perflurobutane for hepatocellular carcinoma surveillance: a multicenter diagnostic trial (SCAN). *Radiology.* 2019;292:638-46.
  31. Choi JY, Lee JM, Sirlin CB. CT and MR imaging diagnosis and staging of hepatocellular carcinoma: Part II. Extracellular agents, hepatobiliary agents, and ancillary imaging features. *Radiology.* 2014;273:30-50.
  32. Kim MJ, Rhee HJ, Jeong HT. Hyperintense lesions on gadoxetate disodium-enhanced hepatobiliary phase imaging. *AJR Am J Roentgenol.* 2012;199:W575-86.
  33. Kim JY, Kim MJ, Kim KA, Jeong HT, Park YN. Hyperintense HCC on hepatobiliary phase images of gadoxetic acid-enhanced MRI: correlation with clinical and pathological features. *Eur J Radiol.* 2012;81:3877-82.
  34. Korenaga K, Korenaga M, Furukawa M, Yamasaki T, Sakaida I. Usefulness of Sonazoid contrast-enhanced ultrasonography for hepatocellular carcinoma: comparison with pathological diagnosis and superparamagnetic iron oxide magnetic resonance images. *J Gastroenterol.* 2009;44:733-41.